One-dimensional Simulation of Heat Structure Melting and Evaporation Under High Heat Flux Condition Using MARS

Geon-Woo Kim [a], Jeong-Hun Lee [a], Hyoung-Kyu Cho [a*], Goon-Cherl Park [a], Kihak Im [b]
[a]*Department of Nuclear Engineering, Seoul National University*
1 Gwanak-ro, Gwanak-gu, Seoul 151-744, Republic of Korea
[b] *National Fusion Research Institute 169-148, Yuseong-gu, Daejeon 305-806, Republic of Korea*
[*]*Corresponding author: chohk@snu.ac.kr*

1. Introduction

The fuel rods of nuclear reactors and plasma facing components of fusion devices can be exposed to high heat flux conditions in case of transient or accident situations. Their thermal responses of high heat flux and managements are the major issues in terms of system integrity. In order to establish the successful application for high heat flux condition, it is necessary to analyze material damage including possible phase change such as melting and evaporation due to high heat flux. In addition, in terms of coolant, water which is widely used for coolant has serious concern in that critical heat flux (CHF) occurrence can degrade the cooling capability and aggravate the integrity of cooling components. For thermal hydraulic analysis, two-phase or CHF phenomena can be well predicted with using multidimensional analysis of reactor safety (MARS) code generally used for nuclear reactor safety analyses. However, MARS code cannot simulate the melting and evaporation of materials under high heat flux or heat generation condition by itself due to the absence of those models. In the present study, therefore, one-dimensional heat conduction calculation module for heat structure melting and evaporation was developed and coupled with MARS to overcome the limitation of material phase change simulation capability in MARS code.

As clarifying the high heat flux problem, plasma facing component of Korean demonstration fusion reactor, K-DEMO [1], was selected. The heat flux condition of transient event for fusion reactor due to plasma disruption whose value of 600MW/m^2 with duration time of 0.1 sec [2] was applied as boundary condition.

2. Melting and evaporation model

In this section, melting and evaporation model were introduced. The governing equation of phase change simulation module is

$$\rho C_p \frac{\partial T}{\partial t} = \frac{\partial}{\partial x}\left(k\frac{\partial T}{\partial x}\right) + Q \qquad (1)$$

where ρ is density, C_p is heat capacity, k is thermal conductivity and Q is volumetric heat source. The governing equation was solved numerically using finite volume method and fully implicit scheme. The melting model was applied by modifying heat capacity C_p and the evaporation model was adopted for modification of boundary conditions and usage of moving boundary with adaptive mesh technique to simulate high heat flux erosion due to evaporation.

2.1 Melting model

The effective heat capacity method [3] was used for melting model. This method defines heat capacity as function of temperature as

$$C_p(T) = \begin{cases} C_{p,solid} & T < T_m \\ L/(T_s - T_m) + C_p(T) & T_m \le T \le T_s \\ C_{p,liquid} & T > T_s \end{cases} \qquad (2)$$

where T_m is melting temperature, T_s is solidification temperature and L is specific latent heat. The region between melting and solidification temperature is called 'mushy zone' [4] and it can simulate melting phenomena as absorbing or discharging heat with including latent heat as shown in figure 1.

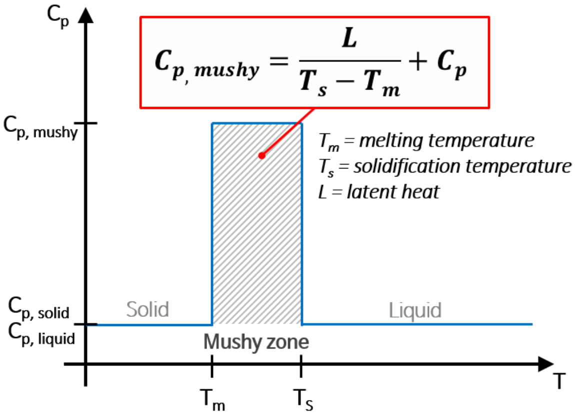

Figure 1. Effective heat capacity method

The validation of melting model was performed in previous study [5] and it showed good agreement with maximum error of 1.34 °C (0.43%).

2.2 Evaporation model

The evaporation model [6] was considered to contain two mechanisms; evaporation and condensation at target surface. First of all, boundary condition on wall where heat flux applied is

$$F(t) = -\mathrm{k}_l(\mathrm{T}_v)\frac{\partial T_l(\mathrm{x})}{\partial x} + \rho_l(T_v)L_v v(t) + \varepsilon\sigma(T_v^{\ 4} - T_0^{\ 4}) \qquad (3)$$

where $F(t)$ is the heat flux of plasma disruption (or possible high heat flux condition), T_v is the temperature of wall surface, T_0 is the temperature of wall not exposed to plasma but in direct line of exposed surface, L_v is the specific latent heat of vaporization, $v(t)$ is the velocity of receding surface, ε is emissivity of wall material, and σ is Stefan-Boltzmann constant. The first term on the right hand side of eq. (3) represents heat flux into wall, the second term is the heat consumed due to vaporization and the last term is radiation heat transfer to cold portion of the wall. The evaporation model is needed to estimate $v(t)$; velocity of receding surface due to evaporation.

According to the theory of Hertz-Knudsen-Langmuir [7] about evaporation and condensation, net flux of atom leaving the surface is

$$J = J_{eq} - J_c = \frac{(\sigma_e P_s - \sigma_c P_c)}{\sqrt{2\pi mkT}} \qquad (4)$$

where J is net evaporation flux, J_{eq} is evaporation flux, J_c is condensation flux, m is mass per atom, k is Boltzmann constant, σ_e and σ_c is coefficient to compensate for non-ideal evaporation or condensation, P_c is ambient partial vapor pressure, and P_s is saturation vapor pressure derived from Clausius-Clapeyron relation as shown below.

$$P_s = P_0 \exp(\frac{L_v}{kT}) \qquad (5)$$

Especially, for the case of evaporation in vacuum condition like fusion reactors, vapor expansion should be considered, therefore, Anisimov and Rakhmatulina [8] suggested that evaporation flux should be defined independently of condensation which arises from physical phenomenon. It is called re-condensation which is due to backscattering of newly vaporized atoms from stagnated vapor right in front of the evaporation surface. The evaporation flux and atom collision frequency in backscattering process are

$$J_e^{\ eq} = \frac{P_s}{\sqrt{2\pi mkT_v}} \qquad (6)$$

$$\frac{1}{\tau_c} = 16\sqrt{2}\pi^{1/3}(\frac{3}{4}\Omega)^{2/3} J_e^{\ eq} \qquad (7)$$

where τ_c represents collision time and Ω is atomic volume. In addition, the relaxation time including re-condensation effect due to backscattering is

$$\tau_R = \frac{20\tau_c}{\ln 10} \cong 10\tau_c \qquad (8)$$

The numerical results of Anisimov and Rakhmatulina suggested the approximated equation for time dependent net evaporation rate as

$$J(\mathrm{t}) = J_e^{\ eq}[0.8 + 0.2\exp(-t/\tau_\mathrm{R})] \qquad (9)$$

Finally, the velocity receding surface due to evaporation is given by

$$v(\mathrm{t}) = \Omega J_e^{\ eq}[0.8 + 0.2\exp(-t/\tau_\mathrm{R})] \qquad (10)$$

2.3 Coupling with MARS and its validation

As MARS has limitation for simulating capability of melting or evaporation, the methodology of code coupling between MARS and phase change simulation module was suggested. The interactive control function [9] and dynamic linked library (DLL) version of MARS were adopted to share information of code interface. The simulation target is first wall of blanket system in K-DEMO fusion reactor and the structure of code modelling is shown in figure 2.

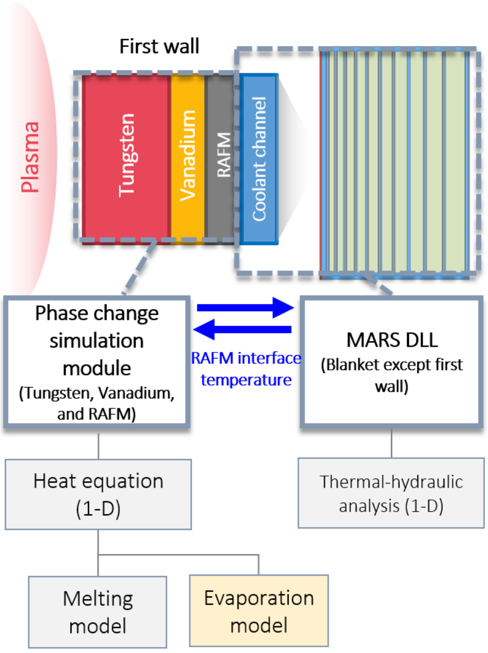

Figure 2. Code coupling between phase change module and MARS DLL and its structure

The validation of code coupling was performed in previous study [5] and it showed good agreement within maximum error of 1.12 °C.

3. Simulation results

The high heat flux condition was derived from plasma disruption event in fusion reactors which has characteristic of extremely high thermal heat flux (hundreds of megawatts per square meter) with short duration time (< 100 ms). The target component of high heat flux is the first wall in blanket, shown in figure 3, which has the function of radiation shielding, cooling, etc. and pressurized water (15MPa, 290℃ inlet) similar with PWR condition is used for coolant. The first wall is composed of tungsten (5mm), vanadium (1mm), reduced activation ferritic/martensitic steel (RAFM; 1mm) and rectangular coolant channel to the direction of away from plasma. The simulation conditions are shown in table I.

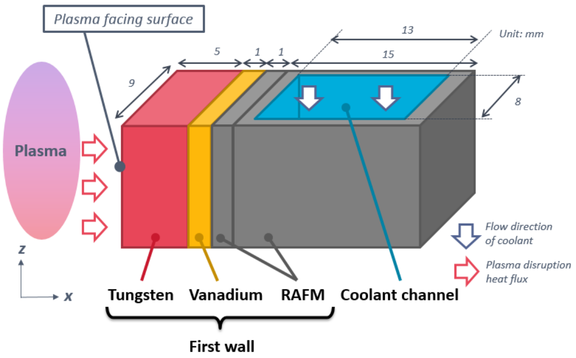

Figure 3. Schematic figure of high heat flux target component; first wall of blanket

Table I. Simulation conditions

Time conditions		
Disruption time		0.1 sec
Time step during disruption		10^{-4} sec
Boundary conditions		
Heat flux	**Before disruption**	0.455 MW/m^2
	Disruption [2]	600 MW/m^2
	After disruption	None

The temperature distributions for x-direction during disruption are shown in figure 4. As high heat flux was applied to plasma facing surface (Fig 3), the temperature of tungsten rapidly soared to about 6300 ℃ at 0.1 sec (end of disruption). At that point, melting layer propagated in depth of about 0.97 mm and tungsten evaporated about 194 μm thick (Fig. 6 and 7). As evaporation proceeded, the heat flux into tungsten wall significantly decreased due to heat consumption of evaporation as shown in figure 8. After the end of disruption, melted tungsten was fully solidified to plasma facing surface (Fig. 6) and evaporation was suddenly terminated. Temperature of first wall cool down and heat was transferred to coolant channel (Fig. 4). As shown in figure 5, heat conduction from front surface (e.g. plasma facing surface) was continued so that heat flux to coolant channel wall exceeded the critical heat flux (CHF). The cooling capability was very poor at that condition so the coolant channel wall temperature rapidly increased but it did not exceed the melting temperature (1500 ℃) of its material, RAFM. The temperature of coolant channel had recovered the that of operation range after about 100 sec. On top of that, first wall component including vanadium and RAFM was not melted except tungsten, that is to say coolant channel was not exposed to plasma which has vacuum pressure.

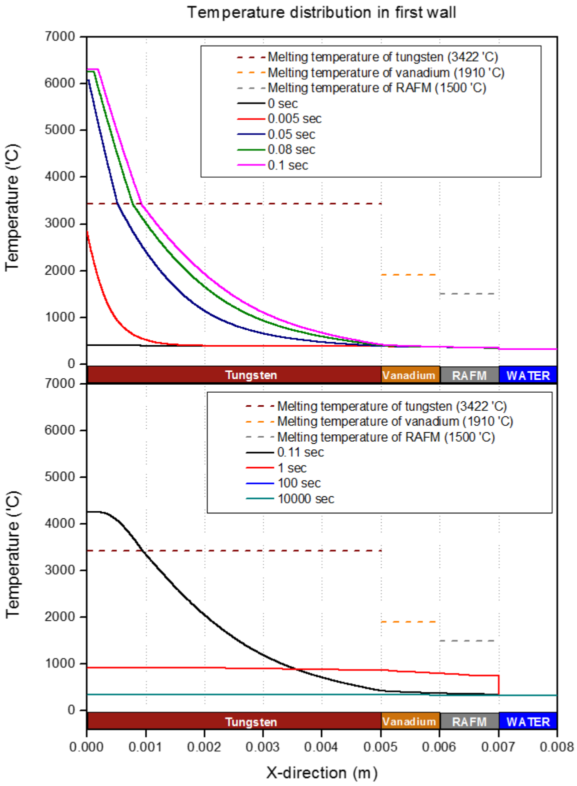

Figure 4. Temperature distribution to x-direction vs. time

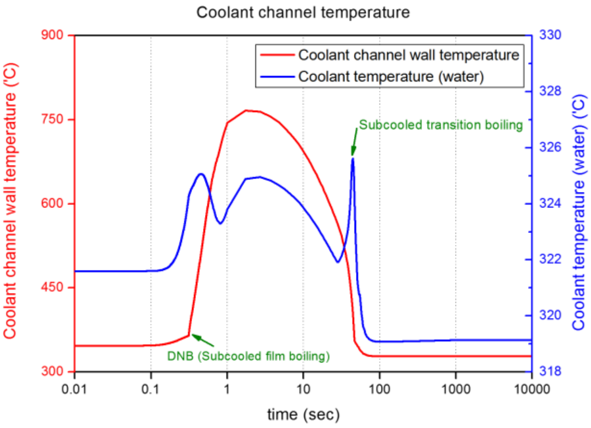

Figure 5. Temperature of coolant and its channel wall

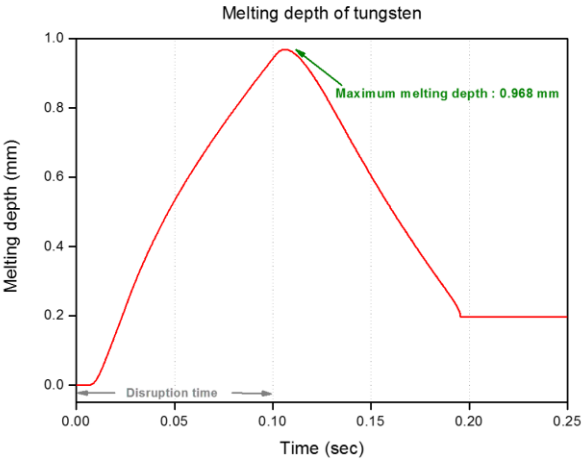

Figure 6. Melting depth of tungsten

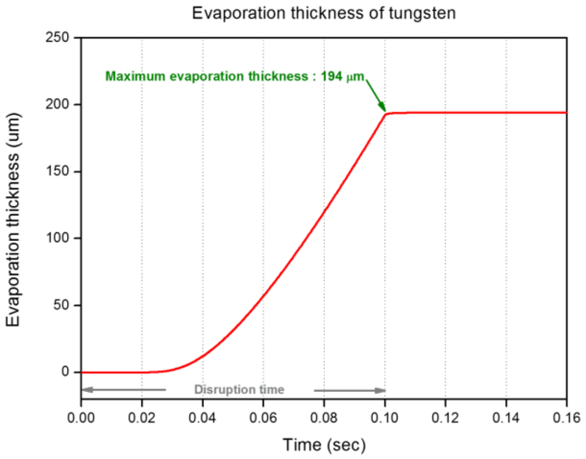

Figure 7. Evaporation thickness of tungsten

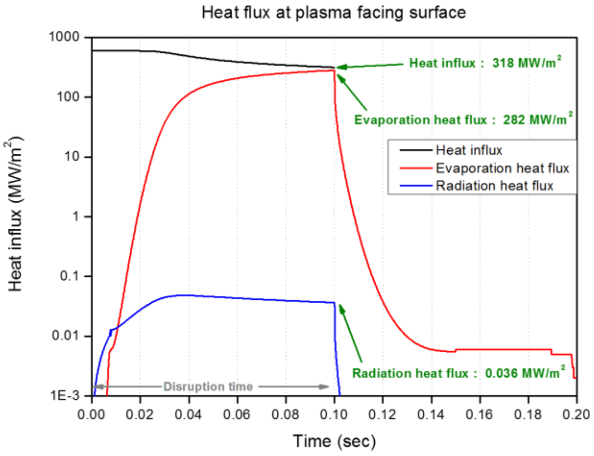

Figure 8. Heat fluxes at plasma facing surface

4. Conclusions

The one-dimensional simulation of melting and evaporation of high heat flux component was performed using MARS and newly developed phase change simulation module. The target component and high heat flux condition were referred to geometry of plasma facing component in Korean fusion demonstration plant and fusion reactor's plasma disruption event. In order to simulate melting and evaporation, effective heat capacity method and evaporation model were applied to phase change simulation module. The simulation results showed several phenomena such as melting, evaporation and CHF occurrence in coolant channel. The proposed phase change simulation module was expected to have wide application to severe accident simulation in nuclear power plant or other transient analysis.

Acknowledgement

This work was supported by R&D Program through the National Fusion Research Institute of Korea (NFRI) funded by the Government funds.

REFERENCES

[1] M. Kwon et al., A strategic plan of Korea for developing fusion energy beyond ITER, Fusion Eng. Des. 83 (2008) 883-888.
[2] A. Cardella, et al., Effects of plasma disruption events on ITER first wall materials, Journal of Nuclear Materials, 283-287, (2000) 1105-1110.
[3] Dariusz Heim, Two solution methods of heat transfer with phase change within whole building dynamic simulation, Ninth International IBPSA Conference, Montreal, Canada, (2005).
[4] W. Ogoh et al., Stefan's problem: validation of a one-dimensional solid-liquid phase change heat transfer process, COMSOL Conference, Boston, USA (2010).
[5] G.W. Kim et al., Phase change of first wall in water-cooled breeding blankets of K-DEMO for vertical displacement events, Korean Nuclear Society Spring Meeting, Jeju, Korea, May 12-13, (2016).
[6] A.M. Hassanein et al., Surface melting and evaporation during disruptions in magnetic fusion reactors, Nucl. Eng. Des. 1 (1984) 307-324.
[7] J. P. Hirth and G. M. Pound, Condensation and evaporation, Progress in Materials Science, Vol 11, Pergamon press (1963) 107.
[8] S.I. Anisimov and A. Kh. Rakhmatulina, The dynamics of the expansion of a vapor when evaporated into a vacuum, Sov. Phys. JETP, vol. 37, No. 3, (1973).
[9] J. J. Jeong et al., Development of a multi-dimensional thermal-hydraulic system code, MARS 1.3.1, Ann. Nucl. Energy 26 (1999) 1611–1642.